Tellus B
Chemical and Physical Meteorology

The Impact of Industrial Activity on the Amount of Atmospheric O_2

ORIGINAL RESEARCH PAPER

MARK O. BATTLE
A. RAINE RAYNOR
STEPHEN E. KESLER
RALPH F. KEELING
*Author affiliations can be found in the back matter of this article

STOCKHOLM UNIVERSITY PRESS

ABSTRACT

Concurrent measurements of atmospheric O_2 and CO_2 amount fractions have been used for decades now to estimate fluxes of carbon to and from the oceans and the land biosphere. The equations used in these estimates explicitly include fossil fuel combustion but are built on the assumption that fossil fuels are oxidized solely by atmospheric O_2, ignoring the small fraction of fossil fuel oxidation by oxide ores that occurs during refining of metals, and thereby overestimating losses of atmospheric O_2. Here, we address this deficiency by quantifying the effective O_2 fluxes associated with the processing of iron, aluminium and copper. We also consider the potential impact of sulfur. We find that consideration of the oxygen mobilized during metal processing (equivalent to a net O_2 flux of $12.0^{+0.2}_{-0.4}$ Tmol a^{-1}) leads to an increased estimate of ocean carbon uptake in the years 2000-2010 of $(0.144^{+0.002}_{-0.005})$ Pg a^{-1} of carbon with a corresponding decrease in estimated land uptake. A rough estimate of oxygen uptake due to sulfur chemistry during fossil fuel combustion (2.4 Tmol a^{-1}) decreases ocean carbon uptake but by a much smaller amount. These corrections are small compared to existing estimates of the fluxes and their uncertainties ((2.27 ± 0.60) and (1.05 ± 0.84) Pg a^{-1} of carbon for ocean and land respectively (Keeling and Manning, 2014)) but should be employed in future analyses.

CORRESPONDING AUTHOR:
Mark O. Battle
Dept. of Physics & Astronomy, Bowdoin College, Brunswick ME 04011-8488, USA
mbattle@bowdoin.edu

KEYWORDS:
Atmospheric oxygen; carbon cycle; industrial atmospheric fluxes; carbon budget

TO CITE THIS ARTICLE:
Battle, MO, Raynor, AR, Kesler, SE and Keeling, RF. 2023. The Impact of Industrial Activity on the Amount of Atmospheric O_2. *Tellus B: Chemical and Physical Meteorology*, 75(1): 65–75. DOI: https://doi.org/10.16993/tellusb.1875

1 INTRODUCTION

Since the pioneering work of Keeling and Shertz (1992), measurements of the abundance of atmospheric O_2 and CO_2 have been used extensively for determining fluxes of carbon to and from the land biosphere and the oceans. The budgets for atmospheric O_2 and CO_2 can be written as

$$\frac{dn(O_2)}{dt} = -\alpha_{ff} F_{ff} - \alpha_B F_{land} + Z_{ocean} \quad (1)$$

$$\frac{dn(CO_2)}{dt} = F_{ff} + F_{land} + F_{ocean} + F_{cem} \quad (2)$$

where n and t are number of moles and time, F_x is the flux of CO_2 from reservoir x to the atmosphere, α_{ff} (is the global average oxidative ratio of fossil fuels, α_B is the effective average oxidative ratio of the global net land carbon sink and Z_{ocean} describes the outgassing of O_2 from the ocean due to warming. F_{cem} represents the CO_2 source associated with the manufacture of cement. α_{FF} varies with time but is roughly 1.4 and α_B is around 1.1 (Keeling and Manning, 2014).

In this paper, we address two shortcomings of Eq. 1: It assumes that atmospheric O_2 is the exclusive oxidant for fossil fuels, and it neglects industrial oxygen fluxes that are not directly linked to fossil-fuel usage. Metal refining violates both of these assumptions. For example, during the refining of iron and aluminium, fossil carbon is oxidized by the oxygen present in hematite, magnetite and alumina, rather than atmospheric O_2. During the refining of copper sulfides, O_2 is removed from the atmosphere, independent of fossil-fuels.

We quantify these effects and correct for them by introducing a term to Eq. 1:

$$\frac{dn(O_2)}{dt} = -\alpha_{ff} F_{ff} - \alpha_B F_{land} + Z_{ocean} + Z_{metals} \quad (3)$$

This allows fossil fuel O_2 losses to be handled as before, with the metal refining being treated as an effective additional source of O_2 to the atmosphere. We then use industrial records to determine annual values of Z_{metals} since 1990. Note that Z_{metals} is only needed for O_2 since the CO_2 flux associated with metal production is already included in equations 2 and 3 in the F_{ff} term.

We further show that O_2 and CO_2 fluxes associated with sulfur are already included conceptually (and approximately) in these budget equations.

We focus on iron, aluminium, copper, and sulfur for two reasons: They are used in great quantities by humanity, and their oxidative states change between extraction and end use. Consequently, they are the heretofore neglected species with the greatest likelihood of influencing the abundance of atmospheric O_2.

In the sections that follow, we treat each species in turn. We briefly describe the path from raw material to refined product and then estimate the quantities of product. From these, we calculate effective fluxes of O_2 to/from the atmosphere. In all cases, we focus exclusively on the raw materials that end up as product and ignore effective fluxes of O_2 associated with oxidation or reduction of raw materials that are extracted but *not* refined, such as mine tailings. We conclude by comparing the effective fluxes from these industrial materials to other terms and uncertainties in the budget.

2 IRON

Iron is an abundant and accessible element, enormously useful in both pure form and alloyed with various other metals as steel. In 2021, world production of iron ore contained about 1.6×10^{12}kg (Tuck, 2022a) of iron, most of which was used to manufacture steel. The ore had a value of roughly $260 billion USD prior to refining (Statista, 2022c). Iron production was more than 25 times as great (by mass) than the next most heavily produced metal: aluminium (Bray, 2020a). With this ubiquity comes the potential for significant fluxes of O_2.

With iron, as with our other species, we determine these fluxes by comparing the oxidative states of the raw and processed materials and scaling by the amount of product. Note that in our accounting, we are *not* concerned with fluxes related to the energy required for production. These are captured in the F_{ff} term in equations 1 and 2.

2.1 PRODUCTION CHEMISTRY

Iron and steel are produced primarily from the important iron-bearing minerals hematite (Fe_2O_3) and magnetite (Fe_3O_4).

At present, the great majority of hematite is turned into iron by reacting the mineral with carbon monoxide in the presence of heat. This strips the oxygen off the iron and turns the CO into CO_2. Although this process typically occurs in three steps, the net reaction is

$$6\,C + 3\,O_2 + 2\,Fe_2O_3 \rightarrow 4\,Fe + 6\,CO_2$$

The carbon in this process typically arrives as coke (derived from coal) which is then partially combusted to form CO.

As written, this reaction shows that 3 moles of O_2 will be required for every 4 moles of iron produced. However, the central question is *where* the O_2 that ends up in CO_2 comes from. Of the 12 oxygen atoms released in CO_2, 6 of them came from the hematite, effectively yielding a source of 3 moles of O_2 to the atmosphere.

The "O_2 source" nature of the process becomes clearer if we recogize that the F_{ff} formulation of Eq. 1 assumes

the oxidant for fossil fuels is exclusively atmospheric O_2. If there is a non-atmospheric oxidant, the equation needs a correction term. In particular, in the reductive refining of metals, the ore itself oxidizes the carbon in the fossil fuel, yielding reduced metal and CO_2 as the products with little or no atmospheric O_2 required. Thus, Eq. 1 overestimates O_2 loss (relative to CO_2 production) whenever oxidized metals are refined using fossil fuel carbon.

As a specific example, consider only the hematite reduction:

$$2\,Fe_2O_3 \rightarrow 4\,Fe + 3\,O_2$$

This immediately shows that producing 4 moles of reduced Fe will release 3 moles of O_2. No matter what the method of hematite processing, because the end product is fully reduced iron, the Fe:O_2 ratio remains 4:3.

Magnetite is processed slightly differently, with Fe_3O_4 and CO reacting to yield FeO and CO_2. The FeO is further reduced with CO to yield pure iron with the following net reaction:

$$4\,C + 2\,O_2 + Fe_3O_4 \rightarrow 3\,Fe + 4\,CO_2$$

Not surprisingly, the Fe:O_2 ratio is 3:2.

2.2 INVENTORY

We use data from the US Geological Survey Mineral Yearbooks (Tuck, 2020a, b) to quantify the global annual production of iron ore from 1990 through 2018. Values are given in Table 1, including both hematite and magnetite. We convert mass of ore to moles of hematite and magnetite by assuming that 80% of the ore is hematite (Tuck, 2019), but as shown below our results are relatively insensitive to this assumption. Using the Fe:O_2 molar ratios of 4:3 and 3:2 respectively yields the source of atmospheric O_2 associated with pig iron production presented in Table 1. A time series of these values is shown in Figure 1.

The details of the fate of iron after it is mined are complicated, with various steps of concentration and refining yielding pig iron and ultimately steel. There are losses along the way, producing substantial quantities of slag and other byproducts. Nonetheless, effectively 100% of the oxidized iron extracted from the earth is reduced (Tuck, 2021), enabling the calculation of the atmospheric O_2 source given above.

In practice, pig iron contains small amounts of carbon, sulfur, silicon, phosphorus and manganese; impurities that are removed as the pig iron is refined into steel. The dominant impurity is carbon, but since it enters the iron from coking coal during smelting its oxidation has been correctly captured by F_{ff} in Eq. 1. Sulfur impurities are also almost entirely introduced by the coking coal, so their oxidation will be described by the treatment of sulfur in fossil fuels (see Sec. 5). Silicon is present in the ore in an oxidized state and remains so during smelting ($SiO_2 + CaO \rightarrow CaSiO_3$). Phosporus and manganese are more complicated, as they are present in mineral ore in an oxidized state, are reduced early in processing, and are then re-oxidized at a later step. Thus, just as with silicon, phosphorus and manganese have no net O_2 flux associated with processing.

We connect these production data to Z_{metals} by the Fe:O_2 ratios given above. For example, if the world produces P moles of reduced iron in a time t and h% of that iron comes from hematite ore, the effective flux of O_2 to the atmosphere will be $Z_{metals_{hematite}} = \frac{3}{4}\frac{hP}{tM_{Fe}}$ where M_{Fe} is the molar mass of iron.

3 ALUMINIUM

Aluminium, the third most abundant element in the earth's crust, is a relative newcomer to human exploitation, first isolated in 1825 and widely used only after 1886 (Kesler and Simon, 2015). The demand for aluminium has grown steadily since then, due to its strength, light weight, and corrosion-resistance, leading to a commercial value second only to iron among metals. Global production in 2021 was 6.8×10^{10} kg (Bray, 2022) with a value of $170 billion USD (Statista, 2022a). Large as this is, the production is only 8% (by mole) of that of iron, implying a relatively modest impact on atmospheric oxygen.

3.1 PRODUCTION CHEMISTRY

Essentially all aluminium extracted for human use comes from bauxite, an ore containing various hydrated aluminium oxides, along with iron and other impurities. The primary oxides are diaspore and böhmite (both AlO(OH)), and gibbsite ($Al(OH)_3$). About 85% of bauxite that is mined is converted to alumina (Al_2O_3) (Merrill, 2022) using the Bayer process of leaching and calcination. The abundances (both relative and total) of AlO(OH) and $Al(OH)_3$ vary substantially from one deposit of bauxite to the next, but these two species have the same oxygen yields during refining. The remaining 15% of the bauxite is used for a variety of purposes but the aluminium in it is not reduced (Bray, 2021).

Of the alumina produced, the great majority (88% in 2017) (Bray, 2020a, b) is reduced to pure aluminium using the Hall-Heroult process. The remaining alumina is not further reduced, and is used instead in chemicals, abrasives and other products (Bray, 2021).

While the Bayer process (converting bauxite to alumina) is quite complicated, the net effect is a partial reduction of the hydrated oxides. Most importantly for our purposes, the liberated oxygen ends up as water. Thus, ignoring links between the oxygen and water cycles, the production of alumina has no impact on atmospheric O_2.

YEAR	WORLD PRODUCTION OF REDUCED IRON (Pg)	ANNUALLY INTEGRATED O_2 SOURCE (Tmol) ASSUMING 80% HEMATITE	ANNUALLY INTEGRATED O_2 SOURCE (Tmol) ASSUMING 50% HEMATITE	ANNUALLY INTEGRATED O_2 SOURCE (Tmol) ASSUMING 95% HEMATITE
1990	0.54	7.09	6.85	7.21
1991	0.52	6.80	6.57	6.92
1992	0.50	6.52	6.30	6.64
1993	0.50	6.52	6.30	6.63
1994	0.51	6.76	6.53	6.88
1995	0.55	7.24	7.00	7.37
1996	0.55	7.18	6.94	7.30
1997	0.59	7.68	7.42	7.81
1998	0.57	7.53	7.27	7.66
1999	0.56	7.35	7.10	7.48
2000	0.60	7.93	7.66	8.07
2001	0.59	7.73	7.46	7.86
2002	0.61	8.07	7.80	8.21
2003	0.64	8.41	8.13	8.56
2004	0.75	9.87	9.54	10.04
2005	0.84	11.07	10.69	11.26
2006	0.96	12.66	12.23	12.87
2007	1.07	14.05	13.57	14.29
2008	1.13	14.84	14.33	15.09
2009	1.09	14.31	13.83	14.56
2010	1.17	15.36	14.84	15.63
2011	1.24	16.28	15.73	16.56
2012	1.26	16.55	15.98	16.83
2013	1.34	17.60	17.00	17.90
2014	1.45	19.04	18.39	19.37
2015	1.46	19.17	18.52	19.50
2016	1.47	19.30	18.65	19.63
2017	1.50	19.70	19.03	20.03
2018	1.52	19.96	19.28	20.30

Table 1 World production of iron and the associated effective release of O_2 to the atmosphere, totalled for each calendar year. While the most likely mix of iron-bearing minerals is 80% hematite and 20% magnetite (by mole), we include other (extreme) scenarios as a sensitivity study. Data from Tuck (2020a).

In contrast, the reduction of alumina to aluminium using Hall-Heroult involves an electrochemical transfer of oxygen from the alumina to carbon from graphite anodes. The consequent release of CO_2 is, once again, effectively a source of atmospheric O_2 since there is oxidation of carbon with no impact on atmospheric O_2 levels. Since the reduction of alumina can be represented as

$$2\,Al_2O_3 \rightarrow 4\,Al + 3\,O_2$$

the ratio of aluminium to O_2 is 4:3.

3.2 INVENTORY

As with iron, we use data from the US Geological Survey Mineral Yearbooks (Bray, 2020a, b) for global annual production of pure aluminium from 1990 through 2017. Values are given in Table 2.

Since there is no O_2 flux associated with the Bayer process, we only need to account for the refining of alumina to aluminium. Applying the 4:3 ratio given above yields the values shown in Table 2 as well as Figure 1.

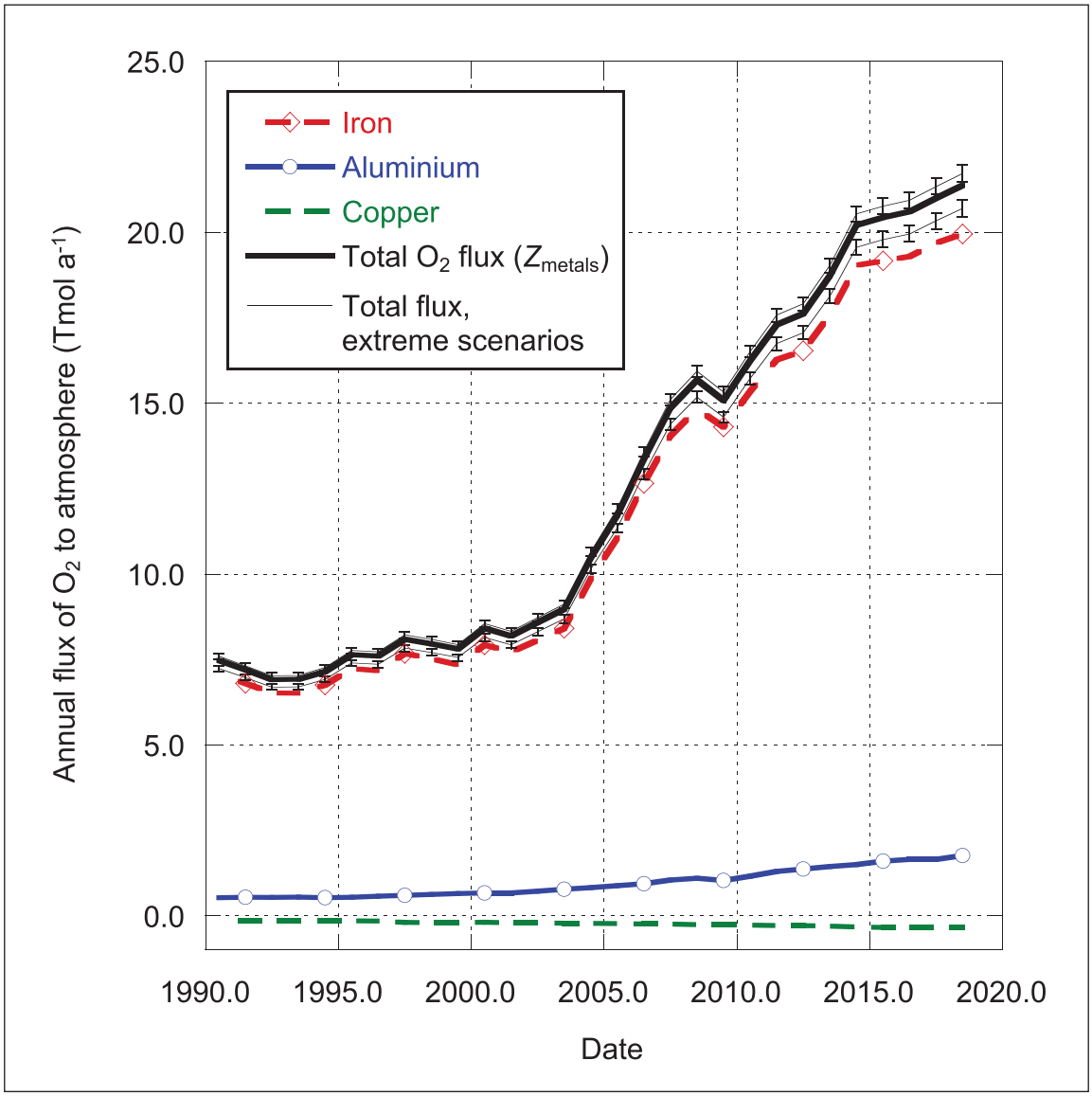

Figure 1 Effective fluxes of O_2 to the atmosphere associated with production of various metals (10^{12} mol a^{-1}). Negative values indicate a flux *from* the atmosphere. We assume iron is derived from 80% hematite and 20% magnetite (by mole). We assume copper is derived exclusively from sulfides. The heavy black line is the best estimate of total effective flux to the atmosphere from all sources (assuming an 80/20 mix of hematite and magnetite). The thin black lines show extreme cases (assuming 95% hematite and 50% hematite). Error bars on the extreme cases show the additional uncertainty (1σ) *not* originating from the unknown hematite/magnetite mix. Values are taken from Table 4, assigning the total annual value to the mid-year point and interpolating linearly.

4 COPPER

Copper was one of the first metals used by humans and played a pivotal role in the development of civilization, first in pure form and later alloyed with tin as bronze. In modern society it remains essential, serving crucial functions in electrical power generation and electronics, plumbing, and marine applications. In 2021, roughly 2.1×10^{10} kg of copper was mined worldwide (Flanagan, 2022). This had a value of roughly $196 billion USD (Statista, 2022b). While these figures clearly show the global importance of copper, the production is only 1.1% of iron (by mole), suggesting a smaller influence on atmospheric oxygen than either iron or aluminium. The quantity of copper recycled and reclaimed is substantial (of order 5×10^9 kg) but its processing does not generate O_2 fluxes, so we ignore it in the work that follows.

4.1 PRODUCTION CHEMISTRY

The chemistry of copper production is more complicated than that of iron and aluminium since some copper-bearing minerals are sulfides while others are oxides. The dominant sulfides and their approximate fractional molar abundances are chalcopyrite ($CuFeS_2$ 70%), chalcocite (Cu_2S 15%) and bornite (Cu_5FeS_4 10%). The oxides are primarily malachite ($Cu_2(CO_3)(OH)_2$), atacamite ($Cu_2Cl(OH)_3$), brochantite ($Cu_4SO_4(OH)_6$) and chrysocolla ($(Cu,Al)_2H_2Si_2O_5(OH)_4 \cdot nH_2O$), all roughly equally abundant (Sillitoe, 2021).

Sulfides account for about 85% of copper production (Schlesinger et al., 2011). Because the sulfides contain

YEAR	WORLD PRODUCTION OF REDUCED ALUMINIUM (Tg)	ANNUALLY INTEGRATED O_2 SOURCE (Tmol) FROM REDUCTION OF ALUMINA
1990	19.3	0.54
1991	19.7	0.55
1992	19.5	0.54
1993	19.8	0.55
1994	19.2	0.53
1995	19.7	0.55
1996	20.8	0.58
1997	21.7	0.60
1998	22.6	0.63
1999	23.6	0.66
2000	24.3	0.68
2001	24.3	0.68
2002	26.1	0.73
2003	28.0	0.78
2004	29.9	0.83
2005	31.9	0.89
2006	33.9	0.94
2007	37.9	1.05
2008	39.7	1.10
2009	37.2	1.03
2010	41.8	1.16
2011	46.8	1.30
2012	49.3	1.37
2013	52.1	1.45
2014	54.1	1.50
2015	57.8	1.61
2016	59.5	1.65
2017	59.5	1.65
2018	63.6	1.77
2019	63.2	1.76

Table 2 World production of aluminium and the associated effective release of O_2 to the atmosphere, totalled for each calendar year. Data from Bray (2020a, b).

no oxygen, they cannot be a source to the atmosphere. Instead, the reduced sulfur and iron liberated during processing are eventually oxidized, functioning as a sink of atmospheric O_2.

Elemental copper in chalcopyrite and bornite is extracted by concentration and smelting, followed by electrolytic refinement. The iron largely ends up in slag as FeO or Fe_2O_3 and the sulfur is emitted as gaseous sulfur dioxide (SO_2). Copper in chalcocite is refined by leaching, followed by solvent extraction and electrowinning (SX-EW). This yields elemental sulfur. Regardless of the mineral type, the extraction method, or the intermediate oxidation state, the sulfur that is liberated nearly always ends up as sulfuric acid with three of the oxygen atoms in the H_2SO_4 coming from gaseous oxygen while the last comes from liquid water (Schlesinger et al., 2011). In the calculations that follow, as with aluminium we ignore any linkage between atmospheric O_2 and the water cycle. For chalcocite this implies a sink of O_2 in the molar ratio 4:3 ($Cu:O_2$). For chalcopyrite and bornite, the ratios are 8:29 and 40:53 respectively, assuming equal amounts of ferric and ferrous oxide in the slag.

An additional complication for the sulfides is the risk of double-counting O_2 fluxes associated with the oxidation of sulfur, since we develop a separate O_2 budget for this element. We choose to include the O_2 sink associated with copper sulfides in the copper budget rather than the sulfur budget, allowing us to limit the sulfur budget calculations to the reduced sulfur present in fossil fuels.

For the copper oxides, elemental copper is produced using the same methods employed for chalcocite, described above (leaching and SX-EW). The chemistry of the leaching is complicated by the variety of oxides to be considered and by the aqueous nature of the process. For example, when a single molecule of malachite is leached (by sulfuric acid), its five oxygens end up in one CO_2 and three water molecules. Rather than try to account for the many possiblities, we simply ignore the small source of atmospheric O_2 originating from processing of copper oxides, recognizing that oxides only account for 15% of copper production which is itself a small fraction of iron production.

4.2 INVENTORY

Again, we use data from the US Geological Survey Mineral Yearbooks (Flanagan, 2021) for global annual production of copper ore from 1990 through 2017. Values are given in Table 3.

We assume 85% sulfides, with the relative mineral species proportions (scaled to 100% abundance) and $Cu:O_2$ ratios given above. Ignoring any O_2 flux associated with the processing of oxides, we obtain the sink of atmospheric O_2 given in Table 3 and shown in Figure 1. We recognize that ignoring oxides leads to a slightly exaggerated atmospheric O_2 sink and discuss this further in Section 6.

5 SULFUR

Sulfur is widely used as an industrial raw material, and is essential in the world's fertilizer and manufacturing sectors. The great majority of sulfur ends up as sulfuric acid, the most abundant inorganic chemical produced in the United States (Apodaca, 2022). The total world production of sulfur in 2017 was 80.2 million metric tonnes (Mt), slightly more than aluminium on a molar basis.

YEAR	WORLD PRODUCTION OF REDUCED COPPER (Tg)	ANNUALLY INTEGRATED O_2 SINK (Tmol) SULFIDES ONLY
1990	8.62	0.15
1991	8.65	0.15
1992	8.73	0.15
1993	8.42	0.14
1994	8.43	0.14
1995	8.49	0.14
1996	9.05	0.15
1997	11.14	0.19
1998	11.40	0.19
1999	11.61	0.20
2000	11.02	0.19
2001	12.11	0.20
2002	12.19	0.21
2003	12.59	0.21
2004	12.81	0.22
2005	13.19	0.22
2006	13.73	0.23
2007	13.88	0.23
2008	15.03	0.25
2009	15.38	0.26
2010	15.85	0.27
2011	16.40	0.28
2012	16.88	0.29
2013	17.74	0.30
2014	19.20	0.32
2015	19.63	0.33
2016	19.96	0.34
2017	19.95	0.34
2018	20.27	0.34

Table 3 World production of copper and the associated *removal* of O_2 from the atmosphere, totalled for each calendar year. We ignore copper produced from oxide minerals. We assume that 70% of the copper (by mole) comes from chalcopyrite, 15% from chalcocite and 10% from bornite (Sillitoe, 2021), with O_2:Cu molar ratios of 29:8, 3:4 and 53:40, respectively. Production data from Flanagan (2021).

Significantly, only about 8% (as of 2017) of the world demand for sulfur is met by "discretionary" production, in which sulfur or iron sulfides (usually pyrite) are mined from discrete deposits (Apodaca, 2022). The remaining 92% of the world demand is met by "nondiscretionary" production: sulfur, sulfur dioxide and sulfuric acid recovered as byproducts of other process. The byproducts have significant commercial value and their abundance has led to almost complete cessation of Frasch-process sulfur mining (Ober et al., 2016).

The dominance of nondiscretionary production is a relatively recent phenomenon. Production of H_2SO_4 from fossil fuels began in the mid-1970s as regulation limited SO_2 emissions. Global emissions of SO_2 peaked at 130 Mt in the late 1980s and have fallen steadily since (Ober et al., 2016). The captured sulfur has almost completely replaced discretionary production. Globally, non-discretionary production now exceeds demand, driving down sulfur prices and leading to growing challenges for storage and disposal (Ober et al., 2016).

Thanks to this transition to non-discretionary production, sulfur is in a different category than iron, aluminium and copper: Current production of sulfur is almost entirely associated with fossil fuel production. This has two consequences. First, the sulfur in fossil fuels is in a reduced state and is subsequently oxidized, serving as a *sink* of atmospheric O_2, much like the copper sulfides discussed above.

Second, we can largely incorporate sulfur directly into the O_2 budget through careful handling of fossil fuel combustion with no need for separate O_2 fluxes in Eq. 1. This was essentially done by Keeling (1988) when he used α_{ff} to characterize the fluxes of O_2 associated with the combuston of non-carbon species present in fossil fuels. At the time of Keeling's work, discretionary sulfur production was substantial. In the years since, it has become negligible, so Keeling's formulation has the potential to completely account for the sulfur-driven sink of atmospheric O_2. In brief, the value of α_{ff} is a consumption-weighted average of α_{gas}, α_{liquid} and α_{solid}. These fuel-specific oxidative ratios are built on the abundance of C, H, S & N in the fuels, assuming (among other things) the sulfur ends up as H_2SO_4. Thus, in Eq. 1, α_{ff} captures the O_2 flux associated with all non-discretionary sulfur production.

In practice, this approach to budgeting has complications that are beyond the scope of this paper. For example, the chemistry of flue gas desulfurization changes both the O_2 and CO_2 fluxes somewhat. It is also possible that the amount of sulfur in the coal, oil and gas reserves currently being exploited is different from those in use nearly 40 years ago. Discretionary production of sulfur is not utterly negligible at 8% of the total. Some sulfur (perhaps 7% of production) is consumed as elemental sulfur (Messick, 2011), rather than being converted to H_2SO_4. Natural gas (essentially CH_4) contains no sulfur, but is very often found with H_2S. The latter is captured pre-combustion and converted to H_2SO_4, consuming O_2. Additionally, correctly characterizing uncertainties is particularly challenging.

While we choose to defer a rigorous calculation, we can make a very rough estimate of the currently-neglected O_2 sink associated with sulfur production. In 2017 world production of sulfur included 17 Tg from metallurgy, 49 Tg from liquid and gaseous fuels, 140 Tg from solid fuels and 13 Tg from sulfides and other

discretionary production (Apodaca, 2022; Gilfillan and Marland, 2021; Keeling, 1988). If we assume each sulfur atom sinks 1.5 O_2 molecules for solid fuels and 2.0 in every other case, this implies a sulfur-driven O_2 sink of 11.5 Tmol in 2017. However, the α_{ff} formulation of Keeling (1988) takes nearly all of the O_2 sink associated with the sulfur in liquid and solid fuels into account. Thus, taking the liquid and solid terms out of this total leaves 39 Tg (1.2 Tmol) of sulfur, removing 2.4 Tmol of O_2 in 2017. We discuss the significance of this residual term in Sec. 6.2 below.

6 RESULTS, UNCERTAINTIES AND DISCUSSION

6.1 METALS

Collectively, Tables 1, 2 and 3 show that the production of useful iron, aluminium and copper from mined minerals resulted in a net annual flux of O_2 to the atmosphere of between 21 and 22 Tmol a^{-1} in 2017, depending on assumptions about the mix of iron species refined into metals. Averaged over the period 2000–2010, the range is 11.6–12.2 with a most likely value of 12.0 Tmol a^{-1}. This flux (Z_{metals}) should be added into Eq. 1. Like all of the other terms in Eqs. 1 and 2, Z_{metals} varies over time. To facilitate incorporation of Z_{metals} in future O_2-based carbon budgets, the total flux shown in Figure 1 is also given (with uncertainties) as Table 4. The uncertainty in these fluxes is difficult to rigorously quantify due to the assumptions involved in their estimation.

The largest uncertainty of which we are aware comes from the hematite/magnetite mix from which iron is refined. While an 80:20 (mol mol^{-1}) mix is our best estimate, we only know with certainty that a majority of iron comes from hematite but *some* comes from magnetite. Thus, we consider 95:5 and 50:50 mixes as extreme cases around our 80:20 central value. These result in an asymmetric range of values for the estimated O_2 flux from iron. In 2018, the effective oxygen release was $(21.37^{+0.34}_{-0.68})$ Tmol O_2.

Luckily, uncertain aspects of the processing of iron (*e.g.* losses to slag and other byproducts as iron ore becomes pig iron, or losses during transport) are irrelevant, as essentially 100% of the iron in the ore is reduced, regardless of whether it ends up in its intended form (Tuck, 2021).

We take the total production figures for iron, aluminium and copper from the USGS, which does not formally calculate uncertainties. Although presented by convention with three significant figures, the global values for iron production are likely good to 0.75% or better (Tuck, 2022c). Global copper production is significantly less certain (roughly 5% for solvent-extraction/electrowinning and 10% for primary smelting (Flanagan, 2022)). We assume similar uncertainty for aluminium (10%). For 2018, these imply uncertainties in the total effective release of O_2 of 0.15, 0.03 and 0.18 Tmol of O_2, respectively.

Our treatment of copper has several additional uncertainties and biases. We assume that iron present in

YEAR	ANNUALLY INTEGRATED O_2 SOURCE (Tmol)
1990	$7.48^{+0.15}_{-0.26}$
1991	$7.20^{+0.14}_{-0.25}$
1992	$6.92^{+0.14}_{-0.24}$
1993	$6.93^{+0.14}_{-0.24}$
1994	$7.15^{+0.14}_{-0.24}$
1995	$7.64^{+0.15}_{-0.26}$
1996	$7.60^{+0.15}_{-0.26}$
1997	$8.09^{+0.16}_{-0.28}$
1998	$7.96^{+0.16}_{-0.27}$
1999	$7.81^{+0.16}_{-0.27}$
2000	$8.42^{+0.17}_{-0.29}$
2001	$8.19^{+0.17}_{-0.28}$
2002	$8.59^{+0.17}_{-0.30}$
2003	$8.98^{+0.18}_{-0.31}$
2004	$10.48^{+0.21}_{-0.36}$
2005	$11.73^{+0.23}_{-0.40}$
2006	$13.36^{+0.26}_{-0.46}$
2007	$14.86^{+0.29}_{-0.50}$
2008	$15.68^{+0.30}_{-0.53}$
2009	$15.08^{+0.29}_{-0.51}$
2010	$16.25^{+0.32}_{-0.55}$
2011	$17.30^{+0.34}_{-0.59}$
2012	$17.62^{+0.34}_{-0.60}$
2013	$18.74^{+0.37}_{-0.64}$
2014	$20.21^{+0.39}_{-0.69}$
2015	$20.44^{+0.40}_{-0.69}$
2016	$20.61^{+0.40}_{-0.70}$
2017	$21.00^{+0.41}_{-0.71}$
2018	$21.37^{+0.42}_{-0.72}$

Table 4 Net effective oxygen release to the atmosphere associated with all metals for each calendar year (*i.e.* the annually integrated value of Z_{metals}). Units are 10^{12} moles (Tmol). Upper and lower uncertainties are the quadrature sum of the variations arising from the hematite/magnetite scenarios and all other errors.

copper sulfides is equally likely to be found in FeO and Fe_2O_3 states, but the true distribution is unknown. We assume an 85:15 split on copper sulfides and oxides, but do not know the uncertainty in that split. Lastly, we completely ignore the roughly 15% that are oxides because of the diversity of oxide minerals and the complexity of the processing. This omission will bias Z_{metals} low.

While our ignorance of uncertainties in copper production is unfortunate, it has little impact on the uncertainty in Z_{metals} simply because production of copper is so much smaller than production of iron. Even if the O_2 fluxes from copper carry a 25% uncertainty (an arbitrary, but very conservative number, allowing for the production uncertainty given above and 23% uncertainty from other sources), the 2018 O_2 consumption due to processing of copper will be known to ± 0.09 Tmol.

Uncertainty in O_2 fluxes from aluminium are driven entirely by uncertainties in production so the value of 0.18 Tmol of O_2 (for 2018) quoted above is the whole story.

We have limited the scope of our study to iron and aluminium oxides and copper sulfides. The oxide ores of copper, manganese, titanium, tin, vanadium and tungsten make negligible contributions to the oxygen budget simply because we refine less of them. However, sulfide ores of zinc, nickel, lead and molybdenum are more widely exploited. In total, the amount of these metals extracted from sulphides is comparable, by mole, to copper sulfides. We also ignore the passive oxidation of iron pyrite (FeS_2) in mine tailings, which may lead to O_2 fluxes comparable to the other sulfides. Our neglect of these various sulphides biases our value of Z_{metals} high (since they are O_2 sinks). Conveniently, this neglected-sulfides bias is in the opposite sense of the aforementioned neglected-oxides bias, though it is about 40% smaller so cancellation is incomplete.

While the list of quantified uncertainties given above is neither rigorous nor exhaustive, it is dominated by a single term: the uncertainty in the hematite-magnetite mix. In 2018, this accounts for 0.51 of the total uncertainty in Z_{metals} of ± 0.57 Tmol a^{-1}. Other years are similar. Furthermore, the uncertainty in Z_{metals} is small compared to other uncertainties in the O_2 budget equations.

Z_{metals} should be compared to the various fluxes already in Eq. 1. During the 2000–2010 period, Keeling and Manning (2014) report annual O_2 fluxes of F_{ff} = (934 ± 56) Tmol a^{-1} and Z_{ocean} = (44 ± 45) Tmol a^{-1}. The inferred net land flux is F_{land} = (96 ± 77) Tmol a^{-1}. Z_{metals} (11.6–12.2 Tmol a^{-1}) is much smaller than F_{ff} and very likely smaller than Z_{ocean}. It is also substantially smaller than the uncertainty in F_{land} (arising from uncertainties in F_{ff}, Z_{ocean} and observed dnO_2/dt (Keeling and Manning, 2014)).

Nonetheless, including Z_{metals} in Eq. 1 gives a more accurate model of the O_2 budget and should be done for O_2-budgeting work going forward. Z_{metals} becomes still more significant when Atmospheric Potential Oxygen ($\delta(APO) \equiv \delta(O_2/N_2) + \alpha_B(y(CO_2)/y(O_2)) + C$, where C is an arbitrary scaling constant and y is the dry mole-fraction of the gas) (Stephens et al., 1998; Ishidoya et al., 2022) is the focus, rather than carbon fluxes. Since Z_{metals} is solely an O_2 flux, it becomes relatively large when other paired fluxes partially cancel.

The APO-based analysis of Keeling and Manning (2014) found ocean and land sinks of (2.72 ± 0.6) and (1.05 ± 0.84) Pg a^{-1} of carbon for the years 2000–2010. Adding Z_{metals} to Eq. 1 and repeating the analysis, the oceanic carbon sink increases by $(0.144^{+0.002}_{-0.005})$ Pg a^{-1} and the land sink decreases equivalently. If we take the average of our extreme values and use half the range as the uncertainty, the ocean and land sinks become (2.86 ± 0.60) and (0.92 ± 0.84) Pg a^{-1} of carbon.

Z_{metals} is perhaps most relevant for the secular trends in δ(APO) and the uptake of heat by the ocean that can be inferred from it. As given by Resplandy et al. (2019) in Table S6, the secular trend of $\delta\ APO_{climate}$ has a measurement uncertainty of 0.54 per meg a^{-1} (where "per meg" is analagous to % but includes a multiplier of 10^6 instead of 10^2 Keeling and Shertz, 1992)). Assuming the atmosphere contains 1.77 × 10^8 Tmol of gas, 20.94% of which is O_2, adding 1 Tmol of O_2 to the atmosphere will change the abundance of O_2 (and by extension, APO) by 0.027 per meg. Applying this relationship, by 2014, Z_{metals}, reached 0.55 per meg a^{-1} and has continued to grow, highlighting the importance of Z_{metals}, in analysis of this type.

Resplandy et al. (2019) also calculated an ocean heat uptake of (1.29 ± 0.79) × 10^{22} J a^{-1} for the years 1991–2015. In this same period, Z_{metals} has an average value of (0.317 ± 0.002) per meg a^{-1}, or (0.368± 0.002) × 10^{22} J a^{-1}, this reduces the inferred heat uptake to (0.92 ± 0.79) × 10^{22} J a^{-1}. The correction is roughly half of the uncertainty in the inferred value, but as a systematic error, it should be applied.

Looking decades or more ahead, our framework for calculating Z_{metals} will likely need adjustment. Efforts are underway to refine iron-bearing minerals at lower temperatures using hydrogen-rich reductants, releasing some oxygen as H_2O rather than CO_2. Bauxite will inevitably be replaced by other aluminium-bearing oxides and silicates. For copper and other base metals, the proportion of sulfide ores will increase as we mine deeper deposits that have not been weathered.

Moving from production to consumption, the reduced state of iron has a finite lifetime in our oxygen-rich atmosphere, leading to a sink of atmospheric O_2. This is very likely a small effect for two reasons. First, the absolute amount of rusting is small. About 85% of steel materials are recycled well before they are fully oxidized (Tuck, 2022b) and much of the steel in exterior use is either formulated as stainless, or is coated periodically to prevent oxidation. Second, iron production in recent decades has grown rapidly (Table 1) causing a large disequilibrium between production and decay that

renders the rust sink negligible. Should iron production stabilize or slow in the future, this correction to Z_{metals} will be worthy of further attention.

6.2 SULFUR

As mentioned in Sec.5, we have chosen to defer a rigorous calculation of the O_2 sink resulting from sulfur oxidation. Much of this sink is already included in Eq. 1 due to the formulation of α_{ff}, but there remains a sink of order 2.4 Tmol a^{-1} that is currently missing.

This value (approximate as it is) should be compared to the 12 Tmol a^{-1} sink represented by Z_{metals}. If we were to introduce Z_{sulfur} = 2.4 Tmol a^{-1} into Eq. 1, it would decrease the ocean carbon sink for 2000–2010 by 0.03 Pg a^{-1} and increase the land carbon sink by the same amount. This is clearly a very small correction to substantially uncertain terms ((2.86 ± 0.60) and (0.92 ± 0.84) Pg a^{-1} for ocean and land, respectively).

Given the small size of the correction and the complexity of a rigorous treatment, we choose to leave a full analysis for later, simply acknowledging that even after including Z_{metals}, all O_2-based ocean carbon sink estimates are biased very slightly high and all O_2-based land carbon sink estimates are biased very slightly low.

ACKNOWLEDGEMENTS

We thank Cristopher Tuck, Joyce Ober, Lee Bray, Daniel Flanagan, Richard Sillitoe, Lori Apodaca, Vincent Camobreco, Christopher Cassar, Gregg Marland and Dennis Gilfillan for helpful conversations and correspondence. Raine Raynor's work was supported by an E.O. LaCasce Jr. Physics Fellowship at Bowdoin College.

COMPETING INTERESTS

The authors have no competing interests to declare.

AUTHOR CONTRIBUTIONS

MB conducted research and wrote the manuscript, RR conducted research, RK posed the problem, SK consulted on the science and all authors reviewed and revised the manuscript.

AUTHOR AFFILIATIONS

Mark O. Battle orcid.org/0000-0001-7318-7329
Dept. of Physics & Astronomy, Bowdoin College, Brunswick ME 04011-8488, USA

A. Raine Raynor
Dept. of Physics & Astronomy, Bowdoin College, Brunswick ME 04011-8488, USA

Stephen E. Kesler
Dept. of Earth and Environmental Sciences, University of Michigan, Ann Arbor, MI 48109, USA

Ralph F. Keeling orcid.org/0000-0002-9749-2253
Scripps Institution of Oceanography, UC San Diego, 9500 Gilman Dr. 0244, La Jolla CA 92093, USA

REFERENCES

Apodaca, L. 2022. 2018 Minerals Yearbook: Sulfur, Tech. rep., U.S. Geological Survey. https://pubs.usgs.gov/myb/vol1/2018/myb1-2018-sulfur.pdf.

Bray, E. 2020a. 2017 Minerals Yearbook: Aluminum [Advance Release], Tech. rep., U.S. Geological Survey. https://d9-wret.s3-us-west-2.amazonaws.com/assets/palladium/production/atoms/files/myb1-2017-alumi.pdf.

Bray, E. 2020b. 2017 Minerals Yearbook: Bauxite and Alumina [Advance Release], Tech. rep., U.S. Geological Survey. https://d9-wret.s3.us-west-2.amazonaws.com/assets/palladium/production/atoms/files/myb1-2017-bauxi.pdf.

Bray, EL. 2021. Personal correspondence.

Bray, EL. 2022. 2022 Mineral Commodity Summary: Aluminum, Tech. rep., U.S. Geological Survey. https://pubs.usgs.gov/periodicals/mcs2022/mcs2022-aluminum.pdf.

Flanagan, D. 2021. 2017 Minerals Yearbook: Copper [Advance Release], Tech. rep., U.S. Geological Survey. https://pubs.usgs.gov/myb/vol1/2017/myb1-2017-copper.pdf.

Flanagan, DM. 2022. 2022 Mineral Commodity Summary: Copper, Tech. rep., U.S. Geological Survey. https://pubs.usgs.gov/periodicals/mcs2022/mcs2022-copper.pdf.

Gilfillan, D and **Marland, G.** 2021. CDIAC-FF: global and national CO_2 emissions from fossil fuel combustion and cement manufacture: 1751–2017. *Earth Systems Science Data*, 13: 1667–1680. DOI: https://doi.org/10.5194/essd-13-1667-2021

Ishidoya, S, Tsuboi, K, Niwa, Y, Matsueda, H, Murayama, S, Ishijima, K and **Saito, K.** 2022. Spatiotemporal variations of the $\delta(O_2/N_2)$, CO_2 and δ(APO) in the troposphere over the western North Pacific. *Atmospheric Chemistry and Physics*, 22: 6953–6970. DOI: https://doi.org/10.5194/acp-22-6953-2022

Keeling, R and **Manning, A.** 2014. Studies of Recent Changes in Atmospheric O_2 Content. In: *Treatise on Geochemistry*, pp. 385–404, Elsevier Inc., 2 edn. DOI: https://doi.org/10.1016/B978-0-08-095975-7.00420-4

Keeling, RF. 1988. Development of an Interferometric Oxygen Analyzer for Precise Measurement of the Atmospheric O_2 Mole Fraction, Ph.D. thesis, Harvard University. http://bluemoon.ucsd.edu/publications/ralph/34_PhDthesis.pdf.

Keeling, RF and **Shertz, SR.** 1992. Seasonal and interannual variations in atmospheric oxygen and implications for the global carbon cycle. *Nature*, 358: 723–727. DOI: https://doi.org/10.1038/358723a0

Kesler, S and **Simon, A.** 2015. Mineral Resources, Economics and the Environment, Cambridge University Press, 2 edn. DOI: https://doi.org/10.1017/CBO9781139871426

Merrill, A. 2022. Bauxite and Alumina Statistics Information, USGS National Minerals Information Center. https://www.usgs.gov/centers/national-minerals-information-center/bauxite-and-alumina-statistics-and-information, retrieved Sept. 12, 2022.

Messick, DL. 2011. World Sulphur Outlook, firt.org/sites/default/files/DonMessick_Sulfur_Outlook.pdf, accessed: 2023-04-28.

Ober, J, Apodaca, L and **Crangle, R, Jr.** 2016. Industrial minerals and sustainability: By-products from SO_2 mitigation as substitutes for mined mineral commodities, in: Geoscience for the Public Good and Global Development: Toward a Sustainable Future, edited by Wessel, G. and Greenberg, J., Special Paper 520, pp. 79–87, The Geological Society of America. DOI: https://doi.org/10.1130/2016.2520(09)

Resplandy, L, Keeling, R, Eddebbar, Y, Brooks, M, Wang, R, Bopp, L, Long, M, Dunne, J, Koeve, W and **Oschlies, A.** 2019. Quantitifcation of ocean heat uptake from changes in atmospheric O_2 and CO_2 composition. *Scientific Reports*. DOI: https://doi.org/10.1038/s41598-019-56490-z

Schlesinger, M, Sole, K and **Davenport, W.** 2011. Extractive Metallurgy of Copper, Elsevier, 5 edn.

Sillitoe, R. 2021. Personal correspondence.

Statista. 2022a. Average prices for aluminum from 2014 to 2025. https://www.statista.com/statistics/675845/average-prices-aluminum-worldwide/, accessed: 2022-09-23.

Statista. 2022b. Average prices for copper worldwide from 2014 to 2025. https://www.statista.com/statistics/675854/average-prices-copper-worldwide/, accessed: 2022-09-23.

Statista. 2022c. Iron ore prices from 2005 to 2021. https://www.statista.com/statistics/282830/iron-ore-prices-since-2003/, accessed: 2022-09-23.

Stephens, BB, Keeling, RF, Heimann, M, Six, KD, Murnane, R and **Caldeira, K.** 1998. Testing global ocean carbon cycle models using measurements of atmospheric O_2 and CO_2 concentration. *Global Biogeochemical Cycles*, 12: 213–230. DOI: https://doi.org/10.1029/97GB03500

Tuck, C. 2020a. 2017. Minerals Yearbook: Iron Ore, Tech. rep., U.S. Geological Survey. https://d9-wret.s3.us-west-2.amazonaws.com/assets/palladium/production/atoms/files/myb1-2017-feore.pdf.

Tuck, C. 2020b. 2017. Minerals Yearbook: Iron and Steel, Tech. rep., U.S. Geological Survey. https://d9-wret.s3.us-west-2.amazonaws.com/assets/palladium/production/atoms/files/myb1-2017-feste.pdf.

Tuck, C. 2022a. 2022 Mineral Commodity Summary: Iron Ore, Tech. rep., U.S. Geological Survey. https://pubs.usgs.gov/periodicals/mcs2022/mcs2022-iron-ore.pdf.

Tuck, C. 2022b. 2022 Mineral Yearbook: Iron and Steel Scrap, Tech. rep., U.S. Geological Survey. https://pubs.usgs.gov/myb/vol1/2018/myb1-2018-urib-steel-scrap.pdf.

Tuck, CC. 2019. Personal correspondence.

Tuck, CC. 2021. Personal correspondence.

Tuck, CC. 2022c. Personal correspondence.

TO CITE THIS ARTICLE:
Battle, MO, Raynor, AR, Kesler, SE and Keeling, RF. 2023. The Impact of Industrial Activity on the Amount of Atmospheric O_2. *Tellus B: Chemical and Physical Meteorology*, 75(1): 65–75. DOI: https://doi.org/10.16993/tellusb.1875

Submitted: 16 November 2023 **Accepted:** 20 November 2023 **Published:** 15 December 2023